Structural and vibrational analyses of 2-(2-benzofuranyl)-2-imidazoline

ARTICLE *in* JOURNAL OF RAMAN SPECTROSCOPY · JANUARY 2011

Impact Factor: 2.67 · DOI: 10.1002/jrs.2659

5 AUTHORS, INCLUDING:

J. J. López González
Universidad de Jaén
134 PUBLICATIONS **1,136** CITATIONS
SEE PROFILE

Silvia A Brandán
National University of Tucuman
123 PUBLICATIONS **895** CITATIONS
SEE PROFILE

Research Article

Journal of RAMAN SPECTROSCOPY

Received: 5 November 2009 Accepted: 24 February 2010 Published online in Wiley Online Library: 14 April 2010

(wileyonlinelibrary.com) DOI 10.1002/jrs.2659

Structural and vibrational analyses of 2-(2-benzofuranyl)-2-imidazoline

C. D. Contreras,[a] M. Montejo,[b] J. J. López González,[b] J. Zinczuk[c†] and S. A. Brandán[a*]

We have studied 2-(2-benzofuranyl)-2-imidazoline (BFI) and characterized it by using infrared and Raman spectroscopies. The density functional theory (DFT) method together with Pople's basis set shows that two conformers exist for the title molecule as have been theoretically determined in the gas phase and that, probably, an average of both conformations is present in the solid phase. The harmonic vibrational wavenumbers for the optimized geometry of the latter conformer were calculated at the B3LYP/6-31G* level in the proximity of the isolated molecule. For a complete assignment of the IR and Raman spectra in the compound in the solid phase, DFT calculations were combined with Pulay's scaled quantum mechanics force field (SQMFF) methodology in order to fit the theoretical wavenumbers to the experimental ones.

Supporting information may be found in the online version of this article.

Keywords: 2-(2-benzofuranyl)-2-imidazoline; vibrational spectra; molecular structure; force field; DFT calculations

Introduction

The structure and activity studies of 2-(2-benzofuranyl)-2-imidazoline (BFI) are of great chemical, biochemical and especially pharmacological importance because it exhibits clinical and therapeutic applications mediated by imidazoline receptors.[1] Thus, this type of compounds interacts with the imidazoline receptors[2–4] in different manners according to their structure.[2] BFI is broadly used in hypertensive therapy because the activities of the furane ring increase when the benzyl group is incorporated into the structure.[5] So far, the structural requirements for imidazoline interaction with the mentioned sites are not clearly understood, and the understanding of the influence of the heterocyclic rings on the compound structure in connection to its relevance in the biological function is essential for the design and synthesis of selective imidazoline ligands. The aim of this work is to carry out an experimental and theoretical study on this compound with quantum chemical methods in order to better understand its structural and vibrational properties. Detailed knowledge of the normal vibrational modes is expected to provide a foundation to understand the conformation-sensitive bands in the vibrational spectra of this interesting molecule. IR and Raman spectral data and theoretical calculations combined with Pulay's scaled quantum mechanics force field (SQMFF) methodology[6–8] were used to carry out a complete and reliable vibrational analysis of the isolated molecule. For that purpose, the optimized geometry and wavenumbers for the normal vibration modes were calculated. In this case, there are no published experimental or high-level theoretical studies on the BFI geometries and force field. Hence, obtaining reliable parameters by theoretical methods is an appealing alternative. The obtained parameters may be used to gain chemical and vibrational insights into related compounds. Moreover, density functional theory (DFT), natural bond orbital (NBO) and topological property calculations were performed to analyze the energies and geometrical parameters of these two conformers in the gas phase as well as the magnitude of intramolecular interactions.

Experimental and Theoretical Calculations

A pure sample of BFI from Aldrich was used. The IR spectrum of the solid was recorded in the wavenumber range from 4000 to 200 cm^{-1} with a Fourier transform infrared (FT-IR) Bruker Vector 22 spectrophotometer, equipped with a Globar source and deuterated triglycine sulfate (DGTS) detector. The data were collected at 1 cm^{-1} resolution and the spectrum was enhanced by the accumulation of 200 scans. The Raman spectrum of the solid compound was recorded between 4000 and 10 cm^{-1} with a Bruker RF100/S spectrometer equipped with an Nd : YAG laser (excitation line of 1064 nm, 800 mW of laser power) and a Ge detector cooled to liquid nitrogen temperature. The spectrum was recorded with a resolution of 1 cm^{-1} and 200 scans.

The potential energy curve associated with rotation around the O11–C10–C2–N3 dihedral angle for the compound with geometry C_1 was studied at the B3LYP/6–31G* level. Two different stable conformations were obtained according to the *anti* and

* *Correspondence to: S. A. Brandán, Cátedra de Fisicoquímica I. Facultad de Bioquímica, Química y Farmacia, Universidad Nacional de Tucumán, San Lorenzo 456, T 4000 CAN, San Miguel de Tucumán, Tucumán, R. Argentina. E-mail: sbrandan@fbqf.unt.edu.ar*

† *Member of the Carrera de Investigador Científico, CONICET, R. Argentina.*

a *Cátedra de Fisicoquímica I. Facultad de Bioquímica, Química y Farmacia, Universidad Nacional de Tucumán, Tucumán, R. Argentina*

b *Departamento de Química Física y Analítica, Facultad de Ciencias Experimentales, Universidad de Jaén, 23071 Jaén, Spain*

c *Instituto de Química Rosario (CONICET-UNR), Facultad de Ciencias Bioquímicas y Farmacéuticas, Santa Fé, R. Argentina*

Journal of RAMAN SPECTROSCOPY

syn positions of the oxygen atom with respect to the N–H bond, named the *anti* and *syn* conformers (Fig. 1). Calculations were performed with the Gaussian 03 program.[9] The structures of the compound were fully optimized by using the hybrid density functional method. In the latter technique, Becke's three functional parameters and the nonlocal correlation provided by Lee–Yang–Parr (B3LYP)[10,11] were used, as implemented in the Gaussian programs. The 6–31G* and 6–311++G** basis sets were used. The structures and labeling of the atoms can be seen in Fig. 1. The electronic charge density topological analysis was performed for both conformers by using the atoms in molecules methodology (AIM)[12] by the AIM200 program package.[13] The NBO calculation was performed using the NBO 3.1[14–17] as implemented in the Gaussian 03 package.[9] The harmonic wavenumbers and the valence force field in Cartesian coordinates were calculated at the B3LYP/6–31G* and 6–311++G** levels of approximation. The resulting force fields were transformed to 'natural' internal coordinates by using the MOLVIB program.[18,19] The natural internal coordinates for BFI have been defined as proposed by Fogarasi *et al*.,[20] while the ring coordinates were defined as in Pulay *et al*.[6–8] and are listed in Table S1 (Supporting Information). Following the SQMFF procedure,[6–8] the harmonic force field for *anti* and *syn* conformers of this compound were evaluated at the B3LYP/6–31G* level. The potential energy distribution (PED) components higher than or equal to 10% were subsequently calculated with the resulting SQM.

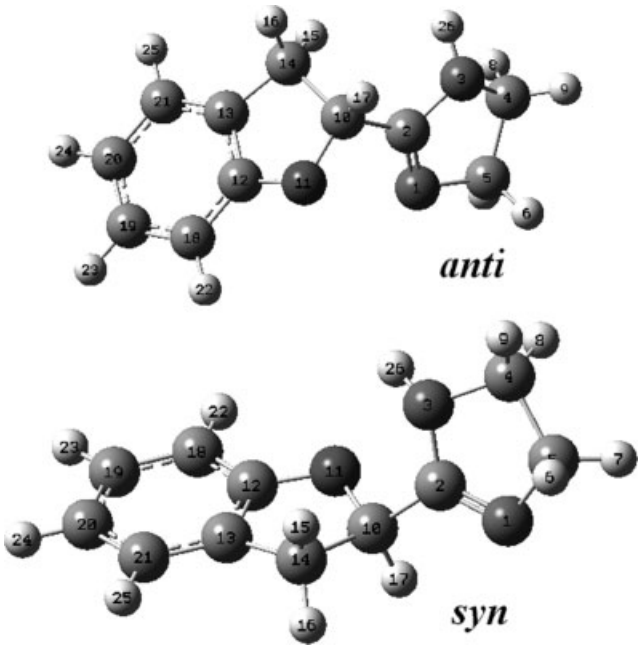

Figure 1. Theoretical structures and atoms numbering for the *anti* and *syn* conformers of 2-(2-benzofuranyl)-2-imidazoline.

Results and Discussion

Geometry optimization

The potential energy curve associated with the rotation around the O11–C10–C2–N3 dihedral angle for the molecule was studied by using the B3LYP method with 6–31G* and 6–311++G** basis sets, presenting in both cases two stable structures (*syn* and *anti*) both of C_1 symmetry. The corresponding structures for both conformers are given in Fig. 1. Table S2 shows the comparison of the total energies and the corresponding dipole moment values for both BFI conformers with the B3LYP method by using different basis sets. Calculations by using the 6–311++G** basis set predict for the *syn* conformer a lower energy value, as can be seen in Table S2. Table 1 shows a comparison of the calculated geometrical parameters for both BFI conformers with those observed from X-ray diffraction corresponding to 2-(2′-furyl)-4,5-1*H*-dihydroimidazole.[21] The theoretical values corresponding to the furane and imidazoline rings for both conformers were compared with the corresponding experimental values of the above-mentioned compound. According to these results, the basis set that best reproduces the experimental geometrical parameters for BFI is 6–311++G** for bond lengths and angles, where the mean difference is 0.027 Å for the *anti* and *syn* conformers, whereas using 6–31G* basis set, the difference in bond lengths between the conformers is 0.002 Å. The inclusion of polarization functions is important to have a better agreement with the experimental geometry. In general, our values are in agreement with the experimental ones for the corresponding imidazoline ring of 2-(2′-furyl)-4,5-1*H*-dihydroimidazole,[21] but for the furane ring there is a significant difference between those values. The calculated C12–O11 bond lengths for both BFI conformers are very different from the observed C–O distance in 2-(2′-furyl)-4,5-1*H*-dihydroimidazole[21] because of the presence of the benzyl and CH_2 groups in the furane ring of BFI. Furthermore, the theoretical calculations by using the 6–311++G** basis set also predict that the two rings in both BFI conformers are not coplanar, with values of ∠C14–C10–C2 between 112 and 114°, whereas in 2-(2′-furyl)-4,5-1*H*-dihydroimidazole[21] this angle has a value of 132.73°. In general, it can be seen that the best results are obtained with B3LYP/6–311++G** calculations, and the introduction of diffuse functions is essential to have closeness to the experimental values, especially in the case of the bond angles.

The stability of the *anti* conformer in relation to the *syn* conformer was investigated by using the electrostatic potential maps[22,23] as in similar molecules.[21,24] The molecular electrostatic potential (ESP) values for both conformers by using 6–31G* and 6–311++G** basis sets are given in Table S3, while the electrostatic potential maps for *anti* and *syn* conformers are shown in Fig. 2. The atomic charges derived from the ESPs (MK)[25] and natural atomic charges were also analyzed and the corresponding values are given in Table S4. Note that both charges are very similar, except the MK charges for both conformers by using 6–311++G** basis set, as also was observed in 2-(2′-furyl)-1*H*-imidazole.[24] The important factor responsible for the lesser stability of the *anti* conformer is the electrostatic repulsion between the two unique pairs on N1 and O11. Hence, a strong red color is observed on both atoms shown in the corresponding Fig. 2. On the other hand, in the *syn* conformer the red color is seen only on the N1 atom of the imidazoline ring. Moreover, the electrostatic repulsion between N1 and O11 is replaced by two possible stabilizing electrostatic interactions between O11 and H26 (distance O11–H26 is 2.442 Å) and N1 and H17 (distance N1–H17 is 2.592 Å). For the *anti* conformer, the dipolar moment value is 3.71 D, while in the syn conformer the dipolar moment is 2.11 D. The bond orders, expressed by Wiberg's index, for the two compound conformers are given in Table S5. We can see that the bond order values for the O11 atom in the *anti* conformer are higher than those corresponding to the other conformer, and also, in both conformers, the bond order values are lower for H26 than

Table 1. Comparison of the calculated geometrical parameters for the conformers of 2-(2-benzofuranyl)-2-imidazoline with the experimental values of the 2-(2′-furyl)-4,5-1*H*-dihydroimidazole molecule

	2-(2-benzofuranyl)-2-imidazoline[a]				2-(2′-Furyl)-4,5-1*H*-dihydroimidazole
	B3LYP/6-31G*		B3LYP/6-311++G**		Experimental[b]
Parameter	*anti*	*syn*	*anti*	*syn*	*anti*
			Bond lengths (Å)		
C12–O11	1.36751	1.39832	1.36621	1.37172	1.369 (3)
C10–O11	1.43868	1.45508	1.44035	1.45953	1.366 (2)
C10–C14	1.56559	1.56070	1.56389	1.55933	1.336 (3)
C14–C13	1.51076	1.51992	1.50966	1.51004	1.413 (3)
C13=C12	1.39546	1.38964	1.39227	1.39352	1.323 (4)
C2=N1	1.27817	1.27929	1.27470	1.27923	1.281 (2)
C5–N1	1.47499	1.50301	1.47560	1.47663	1.472 (3)
C2–N3	1.40192	1.44249	1.39964	1.38959	1.359 (2)
C4–N3	1.47257	1.48783	1.47355	1.47356	1.450 (3)
C4–C5	1.55289	1.55496	1.55022	1.55104	1.518 (3)
			Bond angles (°)		
C12–O11–C10	108.24	106.67	108.47	106.67	105.71 (17)
C14–C10–O11	107.01	108.76	106.72	106.01	110.11 (18)
C10–C14–C13	101.73	101.69	101.65	101.56	106.70 (2)
C14–C13=C12	108.18	108.58	108.20	108.14	106.80 (2)
C12–O11–C10	113.53	114.17	108.47	113.05	110.62 (19)
C14–C10–C2	112.35	112.97	112.32	114.61	132.73 (17)
O11–C10–C2	110.31	108.97	110.73	109.16	117.13 (15)
C2–N1–C5	106.09	106.55	106.41	106.00	105.73 (16)
C2–N3–C4	105.89	104.85	105.87	105.68	106.97 (17)
N1–C2–N3	117.01	117.13	116.57	117.16	116.96 (18)
N3–C5–C4	100.57	102.40	100.39	100.62	101.94 (18)
N1–C4–C5	106.11	106.11	105.68	105.44	106.05 (17)

[a] This work.
[b] Ref [21].

the remaining H atoms. Thus, this atom that belongs to the N–H bond is more labile than the other H atoms, as is expected.

NBO and AIM analyses

The stability of the *anti* conformer of **1** was investigated by NBO calculations.[14–17] The second-order perturbation energies $E^{(2)}$ (donor → acceptor) that involve the most important delocalization are given in Table S6. After a careful analysis of these results, we found that the contributions of the stabilization energies for the $\Delta ET_{\sigma\rightarrow\sigma^*}$ charge transfers of the benzyl group have higher values than the other delocalizations ($\Delta ET_{LP\rightarrow\sigma^*}$) of the remaining rings. On the order hand, the total stabilization energies are approximately similar and, for this reason, it is possible that both conformers exist in solid phase.

Furane, benzyl and imidazoline rings of the molecule have been analyzed by Bader's topological analysis[12] of the charge electron density, $\rho(r)$. The localization of the ring critical point (RCP) in the $\rho(r)$ and the Laplacian values $\nabla^2\rho(r)$ at these points are important for the characterization of molecular electronic structure in terms of the magnitude and nature of the interaction. The RCP is a point of a minimum electron density within the ring surface and a maximum on the ring line.[26] In the case of furane, imidazoline and benzyl rings, the RCP lies in the center of the ring because of symmetry constraints. The values of (ρ) and $\nabla^2\rho(r)$ for the calculated RCP from the topological property analysis for the compound conformers are shown in Table S7. Also, the difference of the basis set on the properties of the RCPs is remarkable in both conformers.

Vibrational Analysis

The recorded infrared and Raman spectra for the compound in the solid phase can be seen in Fig. 3. The two BFI conformers have C_1 symmetries and 72 normal vibration modes, all active in the infrared and Raman spectra. The experimental and calculated wavenumbers for the 72 expected normal vibration modes of both conformers of the studied molecule obtained by using the 6–31G* basis set together with the corresponding assignment are shown in Table 2. The experimental and calculated wavenumbers for the *syn* and *anti* conformers and the corresponding PEDs are given in Tables S8 and S9. In Fig. 3 are included the strong experimental IR and Raman bands, whereas in Table 2 those bands are also highlighted in bold for to facilitate the comparison between the data in the tables and the experimental spectra. Figure 4 shows a comparison between the infrared experimental spectrum of BFI with the calculated infrared spectra for *anti* and *syn* conformers from B3LYP/6–31G* wavenumbers and intensities using Lorentzian band shapes. The populations were calculated with the B3LYP/6–31G* energy difference by using the Boltzmann statistics, for a population relation *syn : anti* of 1 : 1

Journal of RAMAN SPECTROSCOPY

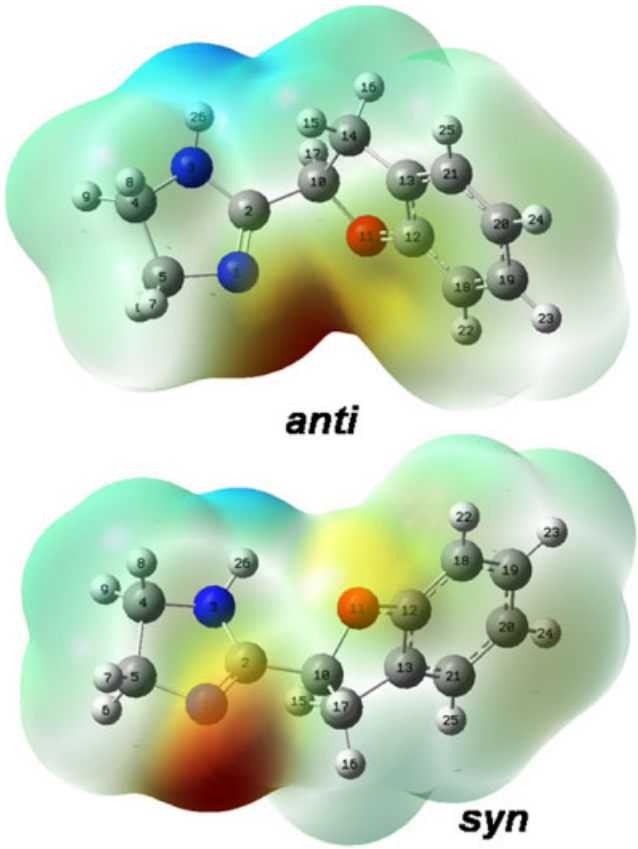

Figure 2. Calculated electrostatic potential surfaces on the molecular surfaces for the *anti* and *syn* conformers of 2-(2-benzofuranyl)-2-imidazoline using the B3LYP functional and 6–31G* basis set. Isodensity value was 0.005. For color ranges see text.

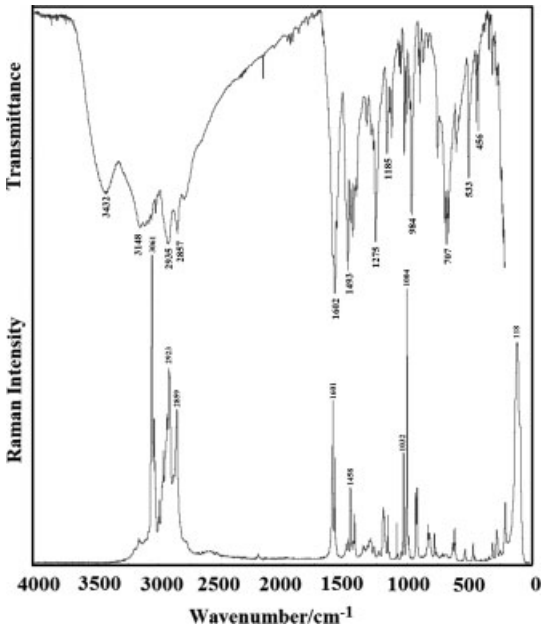

Figure 3. (a) Experimental infrared spectra of the solid 2-(2-benzofuranyl)-2-imidazoline compound; (b) Experimental Raman spectrum.

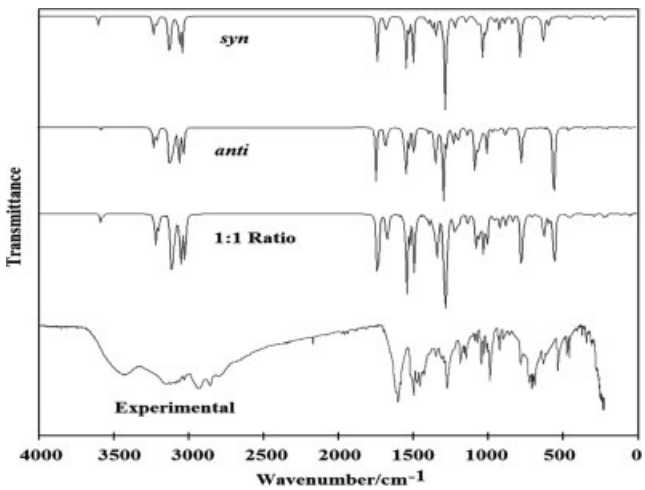

Figure 4. Comparison between the infrared experimental spectrum of 2-(2-benzofuranyl)-2-imidazoline with the calculated infrared spectra for *anti* and *syn* conformers from B3LYP/6–31G* wavenumbers and intensities using Lorentzian band shapes (for a population relation *syn: anti* of 1 : 1 for each conformer).

for each conformer. Thus, the resulting IR spectrum reproduces rather well some bands of the experimental spectrum. The vibrational assignment of the experimental bands to the normal BFI vibrational modes is based on the comparison with related molecules[21,24,27–37] and with the results of the calculations performed here. The theoretical calculations reproduce the normal wavenumbers for the BFI *syn* conformer with initial values of root mean square deviation (RMSD) of 66.7 and 58.4 cm^{-1} by using 6–31G* and 6–311++G** basis sets, respectively, and for the *anti* conformer with initial values of RMSD of 56.9 and 47.3 cm^{-1} by using 6–31G* and 6–311++G** basis sets, respectively. When the SQMFF method is applied by using the Pulay's scaling factors, the final RMSDs for both basis sets slightly decrease to 19.8 and 22.7 cm^{-1} for the *syn* conformer by using 6–31G* and 6–311++G** basis sets, respectively, and to 22.1 and 28.3 cm^{-1} for the *anti* conformer by using the same basis sets, respectively. These results are similar to those obtained for the most stable conformer of 2-(2′-furyl)-4,5-1*H*-dihydroimidazole.[21] The best results for both BFI structures are obtained with the B3LYP/6–31G* calculation because the Pulay's scaling factors are defined for this basis set. We can see in Tables S8 and S9 that only a few modes have participation of $\geq$50% of a single coordinate, whereas the other modes represent very complex vibrations in which several coordinates are involved. The SQM force fields for this compound can be obtained at request. The discussion of the assignment of the most important groups for the studied compound (Tables 2, S8 and S9) is presented below.

Band assignments

NH modes

In accordance with the value reported by Jones and Hirst[30] at 3420 cm^{-1} for the 2,4,5-triphenyl-4,5-dihydroimidazole molecule and at 3434 cm^{-1} in similar compounds,[21,24] the broad band observed in the IR spectra of the compound in the solid phase at 3432 cm^{-1} can be assigned to the N–H stretching vibration in both conformers. The shape of this band shows the spectroscopic signal of an H-bond interaction. For both conformers, the corresponding in-plane deformation mode of this group is assigned to the weak IR band at 1425 cm^{-1} according to the reported value for the 1-benzyl-2-ethylamino-4,5-dihydroimidazole[31] and to theoretical calculations. The out-of-plane deformation mode for the *syn*

Table 2. Observed and calculated wavenumbers (cm^{-1}) using B3LYP method and assignment of 2-(2-benzofuranyl)-2-imidazoline

IR[a]	Raman[b]	SQM[c]	IR int.[d]	Raman act.[e]	SQM[c]	IR int.[d]	Raman act.[e]	Assignment
Solid	Solid		*syn*			*anti*		
3432 s		3430	18.08	71.14	3415	5.10	85.60	ν N–H (*syn, anti*)
3222 sh	3200 vvw	–	–	–	–	–	–	$1602 \times 2 = 3204$
3148 s	3166 vw	3087	9.45	184.52	3092	6.99	153.17	**ν C–H (*syn, anti*)**
3115 s	3115 vvw	–	–	–	3075	30.47	179.83	ν C–H (*anti*)
3084 s	3087 sh	3076	29.89	165.46	3059	17.08	99.78	**ν C–H (*syn, anti*)**
3063 s	**3061 vs**	3061	15.34	108.39	3050	3.02	54.78	**ν C–H (*syn, anti*)**
3046 sh	3044 m	3053	1.14	51.18	2980	45.65	127.18	ν C–H (*syn*), ν_a CH_2 (*anti*)
3031 w	3035 w	2987	19.37	94.22	2970	34.29	122.44	ν_a CH_2 (*syn, anti*)
3007 vw	3006 w	2980	43.72	115.44	2960	32.16	106.40	ν_a CH_2 (*syn, anti*)
2965 sh	2972 w	2971	40.90	149.81	2950	26.81	110.52	ν C–H (*anti*), ν_a CH_2 (*syn*)
2935 vs	**2940 m**	2965	12.82	60.92	2919	25.11	131.19	**ν C–H (*syn*), ν_s CH_2(*anti*)**
–	**2923 s**	2929	15.85	127.54	2917	49.07	138.26	**ν_s CH_2(*syn, anti*)**
–	2886 sh	2912	51.89	131.65	–	–	–	ν_s CH_2 (*syn*)
2857 s	**2859 m**	2895	58.70	123.93	2889	57.69	98.79	**ν_s CH_2(*syn, anti*)**
2170 w	–	–	–	–	–	–	–	H–O
1613 sh	1612 sh	1656	104.30	36.15	1664	77.65	21.11	ν C–C (*syn, anti*)
1602 vs	**1601 s**	1611	13.18	11.78	1612	22.40	11.20	**ν C=N (*syn, anti*)**
1585 sh	1585 m	1599	32.88	13.55	1600	28.54	13.66	ν C–C (*syn, anti*)
1493 s	1496 w	1488	3.08	15.38	1487	1.93	16.69	**δ CH_2(*syn, anti*)**
1493 s	–	1483	94.1	1.21	1484	100.07	1.59	**β C–H (*syn, anti*)**
1473 m	1477 w	1466	2.98	38.96	1467	0.18	29.28	β C–H (*syn, anti*)
1452 m	1458 m	1458	7.09	8.61	1458	0.64	16.45	δ CH_2 (*syn, anti*)
1435 w	1436 w	1446	17.70	14.10	1452	26.95	6.34	δ CH_2 (*syn, anti*)
1425 w	1425 w	1443	96.10	3.99	1436	57.96	1.77	β N–H (*syn, anti*)
1394 sh	–	1363	9.24	6.28	1362	3.73	6.55	Wag CH_2 (*syn, anti*)
1341 w	1355 w	1339	10.76	12.35	1337	9.10	2.87	Wag CH_2 (*syn, anti*)
1338 sh	1321 vvw	1324	24.57	5.66	1331	3.29	9.02	δ O–C–H (*anti*)
1317 sh	–	1315	5.22	4.68	1314	36.53	7.07	Wag CH_2 (*syn, anti*)
1307 w	–	–	–	–	1296	12.67	3.75	β C–H (*anti*)
1291 w	1293 w	1286	33.67	4.40	–	–	–	δ O–C–H (*syn*)
1275 s	1274 sh	1272	10.32	7.26	1258	41.88	7.59	**β C–H (*syn*), ν C–O (*anti*)**
1271 sh	1268 vw	1258	23.36	5.69	1254	132.34	25.57	ρ CH_2 (*syn, anti*)
1232 sh	1229 vvw	1232	94.14	7.06	1236	5.62	5.36	ρ CH_2 (*syn, anti*)
1185 s	1197 w	1223	96.56	26.8	1217	19.99	9.57	δ O–C–H (*anti*)
1185 s	1197 w	1204	14.47	8.39	–	–	–	**ν C–O (*syn*), ν C–C (*syn*)**
1185 s	1189 w	–	–	–	1182	17.76	3.82	ρ CH_2 (*anti*)
1179 sh	–	1181	7.98	9.38	–	–	–	ρ CH_2 (*syn*)
1159 w	1157 w	1167	17.91	2.19	1169	14.70	5.75	ν C–C (*syn*)
1156 sh	–	–	–	–	1160	1.33	5.93	ν C–C (*anti*)
1145 m	1146 vvw	1153	1.42	5.10	1152	12.36	3.87	β C–H (*syn, anti*)
1107 vw	1092 sh	1145	0.83	4.34	1122	13.47	5.71	Twist CH_2 (*syn*), β C–C (*anti*)
1088 w	1087 w	1097	9.42	1.45	1091	8.33	1.29	ν C–C (*syn, anti*)
1073 w	1077 w	–	–	–	1032	7.16	0.95	ν C–N (*anti*)
1048 m	1048 vvw	1030	4.57	0.54	1013	76.70	1.61	ν C–N (*syn, anti*)
1030 m	1032 m	1011	9.94	5.66	1011	18.76	2.03	ν C–C (*syn, anti*)
1007 w	**1004 vs**	1002	3.88	14.87	1004	10.40	14.77	**Twist CH_2(*syn, anti*)**
984 s	985 sh	998	15.48	5.83	993	27.34	7.55	**ν C–O (*syn, anti*), ν C–N (*syn*)**
977 sh	972 vvw	977	69.32	1.20	–	–	–	γ C–H (*syn*)
967 sh	967 vvw	974	17.40	3.90	974	7.82	1.05	ν C–C (*syn*), γ C–H (*anti*)
–	958 vvw	972	36.34	0.56	962	38.55	2.89	$\beta R_1 i$ (*anti*)
934 w	934 w	946	0.01	0.13	945	0.01	0.18	ν C–N (*syn, anti*)
921 m	924 w	930	9.97	5.79	929	5.91	3.84	γ C–H (*syn, anti*)
896 w	–	899	0.91	1.60	909	2.74	2.71	ν C–C (*syn*), twist CH_2 (*anti*)
886 sh	887 vw	873	29.18	7.83	880	7.32	7.55	ν C–C (*anti*)
858 w	–	864	1.52	2.76	863	4.44	2.28	γ C–H (*syn, anti*)

Table 2. (*Continued*)

IR[a]	Raman[b]	SQM[c]	IR int.[d]	Raman act.[e]	SQM[c]	IR int.[d]	Raman act.[e]	Assignment
Solid	Solid		*syn*			*anti*		
849 sh	847 sh	844	9.27	2.65	846	7.13	1.80	βR_1 b (*syn, anti*)
816 sh	824 w	823	3.90	4.00	817	7.84	3.66	Twist CH_2 (*syn*), $\beta R_2 i$ (*anti*)
781 m	783 w	795	12.23	24.69	793	2.39	19.93	βR_1f (*syn, anti*), ν C–C (*syn, anti*)
755 sh	764 vvw	764	25.17	3.01	761	11.30	9.09	γ C–H (*syn, anti*)
740 sh	–	737	71.77	2.90	–	–	–	$\beta R_1 i$ (*syn*)
722 s	–	729	10.08	2.89	735	55.42	0.89	γ C–N (*syn*)
707 s	–	706	1.16	0.57	713	16.80	3.63	**τR_1 b (*syn*), γ C–N (*anti*)**
695 m	694 vvw	–	–	–	705	0.39	1.55	τR_1 b (*anti*)
687 m	–	–	–	–	661	2.31	2.42	Twist CH_2 (*anti*)
631 m	636 vw	639	3.26	0.87	–	–	–	$\beta R_2 i$ (*syn*)
–	622 w	614	4.06	0.63	619	2.54	0.99	βR_2f (*syn, anti*), $Butt_1$ (*anti*)
609 w	614 vw	602	67.12	3.49	588	1.25	4.30	γ N–H (*syn*), βR_3 b (*anti*)
560 vvw	564 vw	592	15.37	3.71	558	0.73	5.84	βR_3 b (*syn*), βR_2 b (*anti*)
549 vvw	551 vvw	564	18.33	7.46	542	70.44	1.33	βR_2 b (*syn*), γ N–H (*anti*)
533 s	534 w	527	3.61	0.72	527	74.83	2.45	**τR_2 b (*syn, anti*)**
472 m	471 w	–	–	–	–	–	–	$118 \times 4 = 472$
456 m	457 vw	–	–	–	–	–	–	$1602 - 1145 = 457$
427 vvw	427 vw	421	4.25	0.88	429	4.95	1.47	δ C–C–C (*syn*), βR_3b (*anti*)
417 vw	413 vw	410	3.46	0.40	411	1.93	0.29	τR_3b (*syn, anti*)
344 w	345 vvw	–	–	–	335	2.59	1.48	τR_1f (*anti*)
312 w	316 w	316	2.84	5.72	–	–	–	ν C–C (*syn*)
285 sh	283 w	–	–	–	289	1.43	1.36	$\tau R_2 i$ (*anti*),
285 sh	277 sh	267	3.19	0.66	–	–	–	τR_1f (*syn*)
257 w	252 vw	264	3.04	1.52	254	0.95	2.55	$\tau R_2 i$ (*syn*), τ C–C (*anti*)
–	247 sh	195	7.26	2.39	197	2.09	2.82	τR_2f (*syn*), $Butt_2$ (*anti*)
–	214 w	186	3.07	2.00	185	3.45	0.63	$Butt_2$ (*syn*), $\tau R_1 i$ (*anti*)
–	**118 vs**	178	1.09	1.27	158	0.05	0.78	**$\tau R_1 i$(*syn*), τR_2f (*anti*)**
–	93 sh	86	2.18	3.66	94	1.40	6.76	$Butt_1$ (*syn*), δ C–C–C (*anti*)
–	–	43	2.61	2.95	33	2.66	2.40	τ C–C (*syn*)
–	–	35	0.13	3.32	23	0.47	4.82	τ C–$C_{inter-ring}$ (*syn, anti*)

Wavenumbers highlighted in bold, see text.
ν, stretching; δ, scissoring; wag, wagging; γ, out-of plane deformation; β, in-plane deformation; ρ, rocking; τ, torsion, twist, twisting; Butt, butterfly; a, antisymmetric; s, symmetric; f, furyl; i, imidazoline; R, ring
[a,b] This work.
[c] From scaled quantum mechanics force field B3LYP/6–31G*.
[d] Units are km mol^{-1}.
[e] Raman activities in $Å^4$ $(amu)^{-1}$.

conformer is assigned to the band at 609 cm^{-1} in the infrared spectrum while for the *anti* conformer is assigned to the observed band at 549 cm^{-1} in the same spectrum. These modes are observed in Raman spectrum at 614 and 551 cm^{-1}, respectively.

The broad band between 2500 and 2200 cm^{-1}, particularly the weak band at 2170 cm^{-1}, can be probably attributed to O–H hydrogen bonding formed by the spatial arrangement of molecules in the lattice crystal, as observed in the molecular packing of the 2-(2′-furyl)-1*H*-imidazole molecule.[24]

CH modes

The group of bands in the 3200–3100 cm^{-1} region in the infrared and Raman spectra of the solid can be assigned to C–H stretching modes. Thus, the strong bands at 3148, 3048 and 3063 cm^{-1} and the shoulder at 3046 cm^{-1} in the IR spectrum can be clearly assigned because of their positions to the four modes for the *syn* conformer, whereas for the other conformer the strong bands at 3148, 3115, 3048 and 3063 cm^{-1} are assigned to such modes. The C–H stretching modes of the C–H bond linked to the C–O bond for the *syn* and *anti* conformers are expected at lower wavenumbers because the C atom presents the sp^3 hybridization, and for this reason those modes are associated with the shoulder and the very strong band at 2965 and 2935 cm^{-1}, respectively. The in-plane deformation modes for the *syn* conformer by using the 6–31G* basis set are clearly calculated at 1483, 1466, 1272 and 1153 cm^{-1} and for the *anti* conformer at 1484, 1467, 1296 and 1152 cm^{-1}; hence, the IR bands at 1493, 1473 and 1145 cm^{-1} are assigned to those modes for both conformers, while the bands at 1307 and 1275 cm^{-1} are assigned to the remaining modes for the *anti* and *syn* conformers, respectively. Taking into account the results of the theoretical calculations and the assignments for similar molecules,[24,27–29] the modes corresponding to out-of-plane deformations of C–H group for both conformers are assigned to the bands at 921, 858 and 755 cm^{-1}, whereas the shoulders at 977 and 967 cm^{-1} are assigned, respectively, to the remaining two modes of the *syn* and *anti* conformers.

CH_2 modes

The three antisymmetric stretching modes of these groups can be assigned to IR bands at 3046, 3031, 3007 and 2965 cm^{-1}, as indicated in Table 2, while their corresponding symmetric modes are assigned to the strong IR bands at 2935 and 2857 cm^{-1} and to the intense band and the shoulder observed in the Raman spectrum at 2923 and 2886 cm^{-1}, respectively. The bands at 3007 and 2935 cm^{-1} are associated with the CH_2 group of the furane ring of the *anti* conformer. The band of medium intensity and the weak band in the IR spectrum, respectively at 1493, 1452 and 1435 cm^{-1}, are clearly assigned to the scissoring modes, in agreement with heterocyclic compounds containing the imidazoline ring,[27–31] while, as the calculation predicted, the bands of medium intensities at 1394, 1341 and 1317 cm^{-1} are easily assigned to the wagging modes. In this case, the bands at 1435 and 1341 cm^{-1} are associated with the CH_2 group of the furane ring. The expected rocking modes are assigned to the medium intensity bands at 1271, 1232, 1185 and 1179 cm^{-1}, while the twisting modes are assigned to the bands at 1107, 1007 and 816 cm^{-1} for the *syn* conformer and at 1007, 896 and 687 cm^{-1} for the *anti* conformer.

Skeletal modes

In this compound, the skeletal stretching modes appear strongly mixed among themselves, as seen in Tables 2, S8 and S9. According to the values reported at 1640 cm^{-1} for 2-(4,5-dihydro-1*H*-imidazol-2-yl)-1*H*-indazole,[31] at 1625 cm^{-1} for 2,4,5-triphenyl-4,5-dihydroimidazole[30] and according to our theoretical results, the strong band at 1602 cm^{-1} is mainly associated with C=N stretching modes. The shoulder and the strong band at 1613 and 1585 cm^{-1}, respectively, are associated with C=C stretching modes of the benzyl ring, while the C–C stretching modes belong to both benzyl and furane rings and they are slightly shifted in relation to those of the furan molecule (1555 and 1490 cm^{-1}).[32] This mode appears strongly coupled in the calculation and with higher a PED contribution at 795 and 794 cm^{-1} for *syn* and *anti* conformers, respectively. For this reason, the IR band of medium intensity at 781 cm^{-1} is assigned to these modes. The three C–N stretching modes for both conformers, as predicted by the calculations, are associated with the bands at 1073, 1048, 984 and 934 cm^{-1}, as can be seen in Table 2. The C–C stretching mode was experimentally observed in the furan molecule at 1385 cm^{-1}. In this compound, since the presence of the benzyl and CH_2 groups in the furane ring is expected, these modes appear at lower wavenumbers. Hence, the bands at 1217 and 1159 cm^{-1} are associated with the vibration normal mode for the *anti* and *syn* conformers, respectively. As predicted by the calculation, the C–C stretching vibrations for the imidazoline ring of the *syn* and *anti* conformers are assigned to the shoulder and the weak IR band at 896 and 886 cm^{-1}, respectively. The strong IR bands at 1275, 1185 and 984 cm^{-1} are assigned to the C–O stretching modes according to the values reported by Klots *et al.*[33] for the furan molecule (1181 and 1067 cm^{-1}). The latter bands are assigned to both conformers. The splitting of these bands is higher for the *anti* conformer (291 cm^{-1}) than for the *syn* conformer (201 cm^{-1}), as expected and in accordance with the difference observed between the values of the corresponding C–O distances presented in Table 1. The three benzyl ring deformations (β_R) are assigned in fluorobenzene,[34] phenylacetylene[35] and phenylsilane[36] between 1000 and 400 cm^{-1}. In the former molecule, the IR bands at 997, 617 and 512 cm^{-1} are associated, respectively, with the β_{R1}, β_{R3} and β_{R2} modes; in the phenylacetylene molecule, the three modes are observed, respectively, at 998, 625 and 463 cm^{-1}, while in phenylsilane those modes are, respectively, assigned at 704, 624 and 388 cm^{-1}. In this case, those modes are calculated for the *syn* conformer with higher PED contribution at 844, 592 and 564 cm^{-1}, respectively, while for the other conformer they are calculated at 846, 588 and 558 cm^{-1}, respectively; for this reason, the IR bands at 849, 609, 560 and 549 cm^{-1} are assigned to those ring deformations. The bands at 849 and 560 cm^{-1} are associated with both conformers. Note that the presence of the furan ring together with the benzyl group reduces the separation among the wavenumbers associated with the β_{R3} and β_{R2} modes. For the same reason, the separation between the two imidazoline ring deformations of the compound notably increases from 43 cm^{-1} (969 and 926 cm^{-1}) for the imidazoline ring deformations of the 2-(2′-furyl)-4,5-1*H*-dihydroimidazole molecule[21] up to approximately 140 cm^{-1} in the BFI molecule. Thus, both imidazoline ring deformation modes are associated with the Raman and IR bands at 958 and 816 cm^{-1}, respectively, for the *anti* conformer and at 740 and 631 cm^{-1} for the *syn* conformer. Taking into consideration the relative position, intensities and the splitting predicted by the calculation, the two furan ring deformations are associated with the bands observed in the IR and Raman spectra at 781 and 622 cm^{-1}, respectively. The three benzyl ring torsions (τ_R) are assigned in fluorobenzene[34] and phenylacetylene[35] between 700 and 300 cm^{-1}. In the former, the IR bands at 685, 500 and 300 cm^{-1} are associated, respectively, with the τ_{R1}, τ_{R2} and τ_{R3} modes, while in phenylacetylene the three modes are assigned, respectively, at 689, 349 and 418 cm^{-1}. In this case, the IR bands at 707, 695, 533 and 417 cm^{-1} are assigned to those ring torsions, where the two last bands are associated with both conformers, as detailed in Table 2. As predicted by the calculation, the two pairs of bands observed in the IR and Raman spectra at 344 and 118 cm^{-1}, respectively, and the shoulders at 285 and 247 cm^{-1} are attributed to the torsion ring modes corresponding to the furane ring of the *syn* and *anti* conformers, respectively, while those corresponding to the imidazoline ring are clearly predicted by calculations at lower wavenumbers. In 2-(2′-furyl)-4,5-1*H*-dihydroimidazole,[21] the torsion ring modes are observed at 304 and 172 cm^{-1}. Hence, they are assigned to Raman bands at 283 and 214 cm^{-1} for the *anti* conformer and at 252 and 118 cm^{-1} for the *syn* conformer. Again, we can see that the effect of the benzyl and CH_2 groups on the furane ring is the displacement of these vibrational modes toward lower wavenumbers. Theoretical calculations predict a higher PED contribution (*ca* 40%) to the C–C inter-ring stretching mode at 388 cm^{-1} for the *anti* conformer of 2-(2′-furyl)-1*H*-imidazole and at 392 cm^{-1} for the *syn* conformer. In this case, this mode is clearly predicted by the calculations for the *syn* conformer at 316 cm^{-1}, while for the other conformer it is predicted to be strongly mixed with other modes at 335 cm^{-1} and with a PED contribution of 8%. Hence, the weak IR band at 316 cm^{-1} is assigned to this mode. The difference in the position of this calculated band is accounted for because in the *syn* conformer the C2–C10 distance is 1.512 Å while in the *anti* conformer it is 1.500 Å, and for this reason such a mode is expected at higher wavenumbers in the latter conformer. On the other hand, the notable repulsion between the N1 and O11 atoms in the *anti* conformer increases the N1–C2–C10–O11 torsion angle and, as a consequence, the corresponding C2–C10 distance is smaller in this conformer. For the studied molecule, in the lower wavenumber region two butterfly modes are expected due to three rings; thus, we designed as $Butt_1$ the torsion between

the furane and imidazoline rings and as $Butt_2$ the torsion between the furane and benzyl rings. These modes are clearly assigned on account of their positions in the Raman spectrum at 622, 247, 214 and 93 cm^{-1}. Here again, we can see that the splitting between both modes is higher for the *anti* conformer than for the *syn* conformer. Probably, this fact is related to the higher value of the N1–C2–C10–O11 torsion angle observed for the *anti* conformer. For reasons already explained, the C–C torsion mode between the furane and imidazoline ring is clearly predicted by the calculation for the *anti* conformer at higher wavenumbers than the *syn* conformer, and it was only possible to assign this mode for the first conformer to the weak IR band at 257 cm^{-1}. For the *syn* conformer, the C–C torsion mode and the C–C torsion inter-ring mode for both conformers were not assigned.

In this compound, both conformers are probably present in the solid phase because the comparison of each vibrational spectra with the corresponding experimental ones are very different between them, whereas, on the contrary, a comparison between the average calculated infrared spectra, as explained before, demonstrates good correlation (Fig. 4). These results are supported by the very strong bands at 1254 cm^{-1} in the calculated IR spectrum for the *anti* conformer and at 1232 cm^{-1} for the *syn* conformer and also by the intense band only observed in the *anti* conformer at lower wavenumbers (527 cm^{-1}), due to their intensities that slightly decrease when the average infrared spectra are calculated; in this way, the resulting spectrum is similar to the experimental one.

Force Field

For the experimentally studied BFI, the corresponding force constants were estimated by using Pulay *et al.*'s[6,7] scaling procedure as mentioned earlier. The force constants expressed in terms of simple valence internal coordinates were calculated from the corresponding scaled force fields by using the MOLVIB program.[18,19] It is interesting to compare the principal force constants, which are collected in Table S10 and calculated at the B3LYP/6–31G* and B3LYP/6–311++G** levels for common vibrations, with those obtained for the 2-(2′-furyl)-4,5-1*H*-dihydroimidazole[21] and 2-(2′-furyl)-1*H*-imidazole.[24] The calculated *f*(C–H), *f*(CH_2), *f*(C–C) and *f*(H–C–H) force constants for both conformers by using the different methods are approximately the same, while the *f*(C–O), *f*(C–N) and *f*(C=N) force constants values are slightly different. These variations are in accordance with the observations presented earlier in the section 'Geometry Optimization and Vibrational Analysis'. Obviously, some force constant values vary in this molecule in relation to 2-(2′-furyl)-4,5-1*H*-dihydroimidazole[21] and 2-(2′-furyl)-1*H*-imidazole.[24] The N–H force constants slightly change according to the corresponding Wiberg bond indexes (Table S5). On the contrary, in all compounds the difference between the force constants of the C=N stretching is remarkable. The *f*(C=N) value changes with the position of the N–H group, being greater in the *anti* conformer than in the *syn* conformer and, moreover, higher in BFI than in the other compounds. The *f*(C–H) force constants are slightly lower in the BFI molecule than in the remaining compounds because in this molecule the calculated values belong to the benzyl group, while in the other two cases they belong to furane and imidazoline rings. Also, the *f*(C–O) force constants for both conformers are different from the reported values for 2-(2′-furyl)-4,5-1*H*-dihydroimidazole[21] and 2-(2′-furyl)-1*H*-imidazole[24] molecules. Here, it is clearly observed that the presence of the benzyl and CH_2 groups in the furane ring of the BFI modifies the properties of that ring and, consequently, the properties of the compound.

Conclusions

The main conclusions of the present paper are the following:

- We have characterized BFI by infrared and Raman spectroscopic techniques in the solid state.
- We have determined the theoretical molecular structure of BFI by the B3LYP/6–31G* and B3LYP/6–311++G** methods and calculations suggest the existence of the stable *syn* conformation in the gas phase and probably both conformations in the solid state.
- The stability of the *anti* conformer of BFI was justified by means of NBO and AIM analyses.
- The average calculated harmonic vibrational wavenumbers for the *anti* and *syn* conformers of BFI are consistent with those in the observed infrared spectrum in the solid state. The presence of both conformers in solid BFI was detected in the IR spectrum and a complete assignment of the vibrational modes was accomplished.
- The SQM force fields were obtained for the *anti* and *syn* conformers of BFI after adjusting the theoretically obtained force constants in order to minimize the difference between the observed and calculated wavenumbers.

Acknowledgements

This work was partially supported by grants from CIUNT (Consejo de Investigaciones, Universidad Nacional de Tucumán) and CONICET (Consejo Nacional de Investigaciones Científicas y Técnicas, R. Argentina). The authors thank Prof. Tom Sundius for his permission to use MOLVIB.

Supporting information

Supporting information may be found in the online version of this article.

References

[1] R. Ten Have, M. Huisman, A. Meetsma, A. M. Van Leusen, *Tetrahedron* **1997**, *53*(33), 11355.
[2] C. Farsang, J. Kapocsi, *Brain Res. Bull.* **1999**, *49*(5), 317.
[3] B. Szabo, *Pharmacol. Ther.* **2002**, *93*, 1.
[4] S. L. F. Chan, C. A. Brown, N. G. Morgan, *Eur. J. Clin. Pharmacol.* **1993**, *230*, 375.
[5] M. Anastassiadou, S. Danoun, L. Crane, G. Baziard-Mouysset, M. Payard, D. H. Caignard, M. C. Rettori, P. Renard, *Bioorg. Med. Chem.* **2001**, *9*, 585.
[6] P. Pulay, G. Fogarasi, F. Pang, E. Boggs, *J. Am. Chem. Soc.* **1979**, *101*(10), 2550.
[7] P. Pulay, G. Fogarasi, G. Pongor, J. E. Boggs, A. Vargha, *J. Am. Chem. Soc.* **1983**, *105*, 7037.
[8] (a) G. Rauhut, P. Pulay, *J. Phys. Chem.* **1995**, *99*, 3093; (b) G. Rauhut, P. Pulay, *J. Phys. Chem.* **1995**, *99*, 14572.
[9] M. J. Frisch, G. W. Trucks, H. B. Schlegel, G. E. Scuseria, M. A. Robb, J. R. Cheeseman, J. A Jr. Montgomery, T. Vreven, K. N. Kudin, J. C. Burant, J. M. Millam, S. S. Iyengar, J. Tomasi, V. Barone, B. Mennucci, M. Cossi, G. Scalmani, N. Rega, G. A. Petersson, H. Nakatsuji, M. Hada, M. Ehara, K. Toyota, R. Fukuda, J. Hasegawa, M. Ishida, T. Nakajima, Y. Honda, O. Kitao, H. Nakai, M. Klene, X. Li, J. E. Knox, H. P. Hratchian, J. B. Cross, C. Adamo, J. Jaramillo,

R. Gomperts, R. E. Stratmann, O. Yazyev, A. J. Austin, R. Cammi, C. Pomelli, J. W. Ochterski, P. Y. Ayala, K. Morokuma, G. A. Voth, P. Salvador, J. J. Dannenberg, V. G. Zakrzewski, S. Dapprich, A. D. Daniels, M. C. Strain, O. Farkas, D. K. Malick, A. D. Rabuck, K. Raghavachari, J. B. Foresman, J. V. Ortiz, Q. Cui, A. G. Baboul, S. Clifford, J. Cioslowski, B. B. Stefanov, G. Liu, A. Liashenko, P. Piskorz, I. Komaromi, R. L. Martin, D. J. Fox, T. Keith, M. A. Al-Laham, C. Y. Peng, A. Nanayakkara, M. Challacombe, P. M. W. Gill, B. Johnson, W. Chen, M. W. Wong, C. Gonzalez, J. A. Pople, *Gaussian 03, Revision B.01*, Gaussian, Inc.: Pittsburgh PA, **2003**.
[10] A. D. Becke, *Phys. Rev.* **1988**, *A38*, 3098.
[11] C. Lee, W. Yang, R. G. Parr, *Phys. Rev. B* **1988**, *41*, 785.
[12] R. F. W. Bader, *Atoms in Molecules, A Quantum Theory*, Oxford University Press: Oxford, **1990**, ISBN: 0198558651.
[13] F. Biegler-Köning, J. Schönbohm, D. Bayles, *J. Comput. Chem.* **2001**, *22*, 545.
[14] A. E. Reed, L. A. Curtis, F. Weinhold, *Chem. Rev.* **1988**, *88*(6), 899.
[15] J. P. Foster, F. Weinhold, *J. Am. Chem. Soc.* **1980**, *102*, 7211.
[16] A. E. Reed, F. Weinhold, *J. Chem. Phys.* **1985**, *83*, 1736.
[17] E. D. Gledening, J. K. Badenhoop, A. D. Reed, J. E. Carpenter, F. F. Weinhold, *NBO 3.1*, Theoretical Chemistry Institute, University of Wisconsin: Madison, WI, **1996**.
[18] T. Sundius, *J. Mol. Struct.* **1990**, *218*, 321.
[19] T. Sundius, *Vib. Spectrosc.* **2002**, *29*, 89.
[20] G. Fogarasi, X. Zhou, P. Taylor, P. Pulay, *J. Am. Chem. Soc.* **1992**, *114*, 8191.
[21] J. Zinczuk, A. E. Ledesma, S. A. Brandán, O. E. Piro, J. J. López-González, A. Ben Altabef, *J. Phys. Chem.* **2009**, *21*, 1.
[22] N. Sadlej-Sosnowska, *J. Phys. Chem. A* **2007**, *111*, 11134.
[23] A. Vektariane, G. S. Vektaris, *ARKIVOC*, **2009**, *VII*, 311.
[24] A. E. Ledesma, S. A. Brandán, J. Zinczuk, O. Piro, J. J. López González, A. Ben Altabef, *J. Phys. Chem.* **2008**, *21*(12), 1086.
[25] B. H. Besler, K. M. Merz Jr, P. A. Kollman, *J. Comp. Chem.* **1990**, *11*, 431.
[26] P. Popelier, *Atoms in Molecules. An Introduction*, Prentice-Hall, Pearson Education Limited: Englewood, NJ, **2000**.
[27] A. E. Ledesma, J. Zinczuk, A. Ben Altabef, J. J. López-González, S. A. Brandán, *J. Raman Spectrosc.* **2009**, *40*(8), 1004.
[28] A. E. Ledesma, J. Zinczuk, J. J. López González, A. Ben Altabef, S. A. Brandán, *J. Raman Spectrosc.* in press, DOI: 10.1002/jrs.2482
[29] A. E. Ledesma, J. Zinczuk, J. J. López González, A. Ben Altabef, S. A. Brandán, *J. Mol. Struct.* **2009**, *924–926*, 322.
[30] R. C. F. Jones, S. C. Hirst, *ARKIVOC* **2003**, *2*, 133.
[31] R. C. F. Jones, J. N. Iley, P. M. J. Lory, *ARKIVOC* **2002**, *6*, 152.
[32] S. T. King, *J. Phys. Chem.* **1970**, *74*, 2133.
[33] T. D. Klots, R. D. Chirrido, W. V. Steele, *Spectrochim. Acta, Part A* **1994**, *50*, 765.
[34] G. Fogarasi, A. G. Császár, *Spectrochim. Acta, Part A* **1988**, *44*(11), 1067.
[35] A. G. Császár, G. Fogarasi, J. E. Boggs, *J. Phys. Chem.* **1989**, *93*, 7644.
[36] M. Alcolea Palafox, *Recent Res. Dev. Phys. Chem.* **1998**, *2*, 213.
[37] P. K. Mallick, G. D. Danzer, D. P. Strommen, J. R. Kincaid, *J. Phys. Chem.* **1988**, *92*, 5628.